



Full length article

## STAT1a and STAT1b of black carp play important roles in the innate immune defense against GCRV

Hui Wu<sup>1</sup>, Yinyin Zhang<sup>1</sup>, Xingyu Lu, Jun Xiao, Pinghui Feng, Hao Feng\*

State Key Laboratory of Developmental Biology of Freshwater Fish, College of Life Science, Hunan Normal University, Changsha, 410081, China

## ARTICLE INFO

## Keywords:

Black carp  
STAT1  
GCRV  
Interferon

## ABSTRACT

Signal transducer and activator of transcription 1 (STAT1) plays an important role in the Janus kinase (JAK)-STAT signaling of human and mammals; however, the mechanism of STAT1 in innate immune activation of teleost fishes remains largely unknown. In this study, two *STAT1* homologues (*bcSTAT1a* and *bcSTAT1b*) of black carp (*Mylopharyngodon piceus*) have been cloned and characterized. Both *bcSTAT1a* and *bcSTAT1b* transcription in host cells was obviously increased in response to the stimulation of poly (I:C), lipopolysaccharide (LPS), grass carp reovirus (GCRV) and interferon (IFN); however, the increase rate of *bcSTAT1b* transcription post stimulation was obviously higher than that of *bcSTAT1a*. *bcSTAT1a* and *bcSTAT1b* were distributed in both cytoplasm and nucleus in the immunofluorescence staining assay. Self-association of *bcSTAT1a* and *bcSTAT1b*, and the interaction between *bcSTAT1a* and *bcSTAT1b* have been detected through co-immunoprecipitation (co-IP) assay; and the data of native polyacrylamide gel electrophoresis (PAGE) implied that *bcSTAT1a* and *bcSTAT1b* might form homodimer and heterodimer *in vivo* like their mammalian counterparts. Both *bcSTAT1a* and *bcSTAT1b* presented IFN-inducing ability in report assay, and both *bcSTAT1a* and *bcSTAT1b* showed antiviral activities against GCRV in EPC cells. Our data support the conclusion that both *bcSTAT1a* and *bcSTAT1b* play important roles in host antiviral innate immune activation initiated by GCRV.

### 1. Introduction

Vertebrates utilize immune system to protect themselves against the invasion of pathogenic microbes, such as viruses, bacteria and fungi, which can be classified into innate immune system and adaptive immune system [1]. Innate immune system provides critical host defence against microorganism invasion through the recognition of conserved pathogen-associated molecular patterns (PAMPs) by pattern recognition receptors (PRRs) [2]. PAMPs are derived from various microbes, such as bacterial LPS, peptidoglycan (PGN), flagellin and lipoteichoic acid (LTA) [2–5]. PRRs, including Toll-like receptors (TLRs), C-type lectin receptors (CLRs), NOD-like receptors (NLRs), RIG-I-like receptors (RLRs) and cytosolic DNA sensors, possess rich diversity and recognize different PAMPs from invading pathogens [6].

Both RLRs and TLRs trigger distinct signaling cascades to activate interferon regulatory factor (IRF) 3/7 (IRF3/7), which translocate to nucleus and trigger the transcription of interferons (IFNs) [2,7]. Mammalian IFNs are classified into type I IFNs, type II IFNs and type III IFNs; all three type IFNs are able to activate the JAK-STAT signaling pathway [8–11]. STAT1 is the hallmark of the JAK/STAT pathway,

which plays an important role in both innate and adaptive immunity. The STAT1 homodimer or heterodimer translocates to nucleus and binds to gamma-activated sequences (GASs) or IFN-stimulated response elements (ISREs) of IFN-stimulated genes (ISGs), and subsequently induces the transcriptional activation of the target ISGs [12–17], which encode numerous cytokines and antiviral proteins. Human (*Homo sapiens*) STAT1 (HsSTAT1) was reported for the first time in 1990 [17], which has two splice variants, named STAT1-alpha (HsSTAT1α) and STAT1-beta (HsSTAT1β) separately [18]. Both HsSTAT1α and HsSTAT1β contain six domains; however, HsSTAT1α but not HsSTAT1β contains complete transcription activation domain (TAD).

To date, *STAT1* homologues have been cloned and characterized from several species in teleost. *STAT1* transcription has been examined in several species, such as Atlantic salmon (*Salmo salar*), orange-spotted grouper (*Epinephelus coioides*), rainbow trout (*Oncorhynchus mykiss*), olive flounder (*Paralichthys olivaceus*), annual fish (*Nothobranchius guentheri*), crucian carp (*Carassius auratus*), malabar grouper (*Epinephelus malabaricus*) and zebrafish (*Danio rerio*) [19–32]. The protein expression of STAT1 has been examined in Atlantic salmon and spotted green pufferfish (*Tetraodon nigroviridis*) [33,34]. Among the

\* Corresponding author.

E-mail address: [fenghao@hunnu.edu.cn](mailto:fenghao@hunnu.edu.cn) (H. Feng).<sup>1</sup> These authors contributed equally to this paper.

above teleost fishes, only a single *STAT1* gene has been cloned except zebrafish. Similarly, zebrafish has two *STAT1* genes related to *HsSTAT1*. Zebrafish *STAT1a* (*DrSTAT1a*) possesses the complete TAD as *HsSTAT1a*, and *DrSTAT1b* contains incomplete TAD as *HsSTAT1β*. Previous report in zebrafish demonstrated that *DrSTAT1a* was transcribed ubiquitously at a low level, however, *DrSTAT1b* showed strong and restricted expression throughout the embryo [27,35].

Black carp is an economically important freshwater species and among the “four famous domestic fishes” in china, which is subjected to bulk of pathogenic microorganisms in natural and aquaculture condition, such as GCRV. However, its innate immune system remains largely unknown. In our previous studies, antiviral protein MX1 and viperin of black carp have been cloned and characterized, which are down-stream ISGs of JAK-STAT pathway [36]. In this paper, two isoforms of black carp *STAT1*, *bcSTAT1a* and *bcSTAT1b*, have been cloned and characterized. Both *bcSTAT1a* and *bcSTAT1b* transcription in *Mylopharyngodon piceus* kidney (MPK) cells were obviously increased in response to different stimuli, however, the increase rate of *bcSTAT1b* mRNA level post stimulation was greatly higher than that of *bcSTAT1a*. Both *bcSTAT1a* and *bcSTAT1b* possess IFN-inducing ability and antiviral activities against GCRV. To our knowledge, this is the first report to show the interaction and functional comparison of two *STAT1* isoforms in teleost fishes, which is important for the further exploration of JAK-STAT signaling of teleost fishes.

## 2. Materials and methods

### 2.1. Cells and plasmids

HEK293T, *epithelioma papulosum cyprini* (EPC) cells, *Ctenopharyngodon idella* kidney (CIK) cells and MPK cells were kept in the lab [37]. All the cell lines were grown in DMEM supplemented with 10% fetal bovine serum, 2 mM L-glutamine, 100 units/ml penicillin and 100 mg/ml streptomycin. HEK293T cells were cultured at 37 °C with 5% CO<sub>2</sub>. EPC, CIK and MPK cells were cultured at 26 °C with 5% CO<sub>2</sub>.

pcDNA5/FRT/TO (Invitrogen; USA), pRL-TK, Luci-bcIFN $\alpha$  (for black carp IFN $\alpha$  promoter activity analysis) and Luci-DrIFN $\phi$ 3 (for zebrafish IFN $\phi$ 3 promoter activity analysis) were kept in the lab [37]. The recombinant expression vector pcDNA5/FRT/TO-bcSTAT1a-HA, pcDNA5/FRT/TO-bcSTAT1b-HA, pcDNA5/FRT/TO-bcSTAT1a-Flag and pcDNA5/FRT/TO-bcSTAT1b-Flag were constructed by cloning the coding sequence (CDS) of bcSTAT1a (bcSTAT1b) fused with an HA (Flag) tag at its C-terminus into pcDNA5/FRT/TO respectively.

### 2.2. Cloning of *bcSTAT1a* and *bcSTAT1b*

Degenerate primers (Table 1) were designed to amplify the CDSs of *bcSTAT1a* and *bcSTAT1b* based on the sequences of *STAT1* of zebrafish, crucian carp and grass carp (*Ctenopharyngodon idellus*). Total RNA was isolated from the spleen of black carp and the first-strand cDNA was

synthesized by using the Revert Aid First Strand cDNA Synthesis Kit (Thermo; USA). The CDSs of *bcSTAT1a* and *bcSTAT1b* were cloned into pMD18-T vector and sequenced by Invitrogen.

### 2.3. Enzyme-linked immunosorbent assay (ELISA)

The bcIFN $\alpha$ -containing conditioned media was measured through ELISA assay as previously described [38]. Briefly, 96-well plate was coated with bcIFN $\alpha$ -containing conditioned media and blocked with carbonate buffer (pH = 9.6) at 4 °C for overnight. After three times of wash, each well was probed with anti-HA antibody (Sigma; USA) at different concentration and cultured at 37 °C for 2 h. After five times of wash, each well was probed with goat-anti mouse secondary antibody (1:30000, Sigma) at 37 °C for 1 h. Then, each well was added with 200  $\mu$ l PNPP for 20 min and 50  $\mu$ l NaOH was added to terminate the exposure. The OD value at 410 nm was measured by Synergy-2 Multimode reader (BioTek; USA).

### 2.4. Quantitative real-time PCR

The primers of quantitative real-time PCR (q-PCR) for *bcSTAT1a*, *bcSTAT1b* and  $\beta$ -actin (as internal control) were listed in Table 1. The mRNA levels of *bcSTAT1a* and *bcSTAT1b* in MPK cells were examined by q-PCR analysis. The program of q-PCR was: 1 cycle of 95 °C/10 min, 40 cycles of 95 °C/15 s, 60 °C/1 min, followed by dissociation curve analysis (60 °C-95 °C) to verify the amplification of a single product. The threshold cycle (CT) value was determined by using the manual setting on the 7500 Real-Time PCR System (ABI; USA) and exported into a Microsoft Excel Sheet for subsequent data analyses where the relative expression ratios of target gene in treated group versus those in control group were calculated by  $2^{-\Delta\Delta CT}$  method.

### 2.5. Virus production and titration

GCRV (strain: GCRV106) was kept in the lab, which was propagated in CIK cells at 26 °C in the presence of 2% fetal bovine serum. Virus titer was examined by plaque assay on EPC cells as previously described [38]. Briefly, the 10-fold serially diluted virus was added onto EPC cells and incubated for 2 h at 26 °C. The supernatant was removed after incubation and fresh DMEM containing 2% FBS and 0.75% methylcellulose (Sigma) was added. Plaques were counted at day-3 post infection.

### 2.6. Immunoblot (IB) assay

HEK293T cells or EPC cells in 6-well plate ( $1.2 \times 10^6$  cells/well) were transfected with pcDNA5/FRT/TO-bcSTAT1a-HA, pcDNA5/FRT/TO-bcSTAT1b-HA or empty vector separately. IB assay was performed as previously described [38]. Briefly, the whole cell lysate was isolated by 8% SDS-PAGE and the transferred membrane was probed with mouse monoclonal anti-HA antibody (1:3000; Sigma) or with rabbit

**Table 1**  
Primers used in the study.

Primer name	Sequence (5′-3′)	Amplicon length (nt) and primer information
bcSTAT1a-C-F	ACTGACGGTACCGCCACCATGAGTCAGTGGTTGGAGCT	Gene cloning
bcSTAT1a-C-R	ACTGACCTCGAGCTCATTTGGTGGACACATACT	
bcSTAT1b-C-F	ACTGACGGTACCGCCACCATGGCACTTTGGAACCCAGCTG	Gene cloning
bcSTAT1b-C-R	ACTGACCTCGAGACACTTTTGGAGTCTTGAAC	
CMV-F	CGAAATGGGCGGTAGGCGTG	
BGH-R	TAGAAGGCACAGTCGAGG	
bc-Q-actin-F	TGGGCACTGCTGCTTCT	q-PCR
bc-Q-actin-R	TGTCGGTCAGGCAGCTCAT	
bcSTAT1a-Q-F	GGAGAACGAGTCCCTGGC	q-PCR
bcSTAT1a-Q-R	TTCTCTTGATCTTGGCG	
bcSTAT1b-Q-F	CCGTCGCAAGTAATGTATC	q-PCR
bcSTAT1b-Q-R	CCTGGAAGTGCTCTGT	

monoclonal anti-HA antibody (1:1000; Sigma), then followed by the incubation with the goat anti-mouse IgG (1:30000; Sigma). The target proteins were visualized with BCIP/NBT Alkaline Phosphatase Color Development Kit (Sigma).

### 2.7. Immunofluorescence microscopy

HEK293T cells and EPC cells in 24-well plate ( $3 \times 10^5$  cells/well) were transfected with pcDNA5/FRT/TO-bcSTAT1a-HA or pcDNA5/FRT/TO-bcSTAT1b-HA separately. The transfected cells were fixed with 4% paraformaldehyde at 24 h post transfection and permeabilized with triton X-100 (0.2% in PBS). After incubated with primary and secondary antibodies, the cells were analyzed by immunofluorescence microscopy as previously described [39]. Mouse monoclonal anti-HA antibody was used at the dilution ratio of 1:400 and Alexa 594-conjugated secondary antibody (Invitrogen) was diluted at 1:800; DAPI was used for nucleus staining.

### 2.8. Co-immunoprecipitation

HEK293T cells in 10 cm dish ( $6 \times 10^6$  cells/well) were co-transfected with pcDNA5/FRT/TO-bcSTAT1a-HA and pcDNA5/FRT/TO-bcSTAT1a-Flag, pcDNA5/FRT/TO-bcSTAT1a-HA and pcDNA5/FRT/TO-bcSTAT1b-Flag, or pcDNA5/FRT/TO-bcSTAT1b-HA and pcDNA5/FRT/TO-bcSTAT1b-Flag separately. For each transfection, the total amount of plasmid DNA was balanced with the empty vector. The transfected cells were harvested at 48 h post-transfection and lysed for immunoprecipitation (IP) assay as previously described [39]. The whole cell lysate of the transfected cells was incubated with protein A/G agarose beads at 4 °C for 2 h. Anti-Flag-conjugated protein A/G agarose beads were added in the supernatant after pre-clearing and incubated with the supernatant media at 4 °C for 4 h. The anti-Flag-conjugated protein A/G agarose beads were boiled in  $2 \times$  sample buffer after 3 times of wash and the eluted proteins were used for IB as above.

### 2.9. Native PAGE

HEK293T cells in 10 cm dish ( $6 \times 10^6$  cells/well) were transfected with pcDNA5/FRT/TO-bcSTAT1a-Flag, pcDNA5/FRT/TO-bcSTAT1b-Flag or empty vector separately. The transfected cells were harvested at 48 h post-transfection and lysed for immunoprecipitation (IP) assay as above method. The proteins bound to anti-Flag-conjugated protein A/G agarose beads were eluted through competitive binding by Flag peptide (Sigma). The eluted proteins were separated on an 8% non-denaturing polyacrylamide gel in the Tris-Glycine native PAGE running buffer (pH = 8.8; without SDS) and the transferred membrane used for IB as above.

### 2.10. Luciferase reporter assay

EPC cells in 24-well plate ( $3 \times 10^5$  cells/well) were co-transfected with pcDNA5/FRT/TO-bcSTAT1a-HA or pcDNA5/FRT/TO-bcSTAT1b-HA, pRL-TK (25 ng/well), and Luci-DrIFN $\phi$ 3 or Luci-bcIFNa (200 ng/well). For each transfection, the total amount of plasmid DNA was balanced with the empty vector. The cells were harvested and lysed on ice at 24 h post transfection. The centrifuged supernatant was used to measure firefly luciferase and renilla luciferase activities according to the instruction of the manufacturer (Promega; USA) as previous reference [37].

### 2.11. Statistics analysis

For the statistics analysis in q-PCR, luciferase reporter assay and viral titer measurement, all data were obtained from three independent experiments with each performed in triplicate. Error bars represented the standard error of the mean value (+SEM) of three independent

experiments. Asterisks (\*) on the pillar marked the significant difference between experimental data and control data (\*p < 0.05; \*\*p < 0.01). The data were analyzed by two-tailed Student's t-test.

## 3. Results

### 3.1. Molecular cloning and sequence analysis of bcSTAT1

The CDS of *bcSTAT1a* consists of 2400 nucleotides (NCBI accession number: MH410166) and the predicted bcSTAT1a protein contains 800 amino acids. The CDS of *bcSTAT1b* consists of 2157 nucleotides (NCBI accession number: MF497810.1), which encodes a polypeptide of 719 amino acids. The calculated molecular weight of bcSTAT1a and bcSTAT1b are 92.3 kDa and 82.9 kDa separately. The theoretical isoelectric points of bcSTAT1a and bcSTAT1b are 5.65 and 5.58 separately (predicted by the ProtParam tool [<http://web.expasy.org/protparam/>]). Amino acid alignment shows that both bcSTAT1a and bcSTAT1b contain six domains: N-terminal domain, coiled-coil domain, DNA binding domain, linker domain, Src homology 2 (SH2) domain and TAD domain, which are similar to HsSTAT1 and DrSTAT1. bcSTAT1a contains the complete TAD and bcSTAT1b only possesses a partial TAD, which is also seen in HsSTAT1 and DrSTAT1 (Fig. 1A).

To gain insight into STAT1 evolution, amino acid sequences of bcSTAT1a and bcSTAT1b have been subjected to multiple alignments with those of STAT1 proteins from different species. Phylogenetic analysis of STAT1s from the selected species demonstrates that these STAT1 homologues could be divided into four groups, consisting of mammals, aves, amphibia and fish branches (Fig. 1B). bcSTAT1a shares high amino acid sequence similarity with DrSTAT1a (86.1%) (Table 2). bcSTAT1b shares high amino acid sequence similarity with STAT1 of crucian carp (99%) and grass carp (98.9%) (Table 2).

### 3.2. bcSTAT1 expression in vitro in response to different stimuli

To investigate the transcription of *bcSTAT1a* and *bcSTAT1b* during innate immune activation, MPK cells were stimulated with poly (I:C), LPS, GCRV or black carp IFNa (bcIFNa) separately, and then used for q-PCR analysis. In the poly (I:C) treated MPK cells, the transcription of both *bcSTAT1a* and *bcSTAT1b* increased right after stimulation. The overall trend of the transcription of both *bcSTAT1a* and *bcSTAT1b* were initially elevated and then decreased (Fig. 2A&B). The highest relative *bcSTAT1a* mRNA level (50  $\mu$ g/ml group, 24 h point) within 48 h post stimulation was 16.3-fold of that of control (without treatment) and the highest relative *bcSTAT1b* mRNA level (25  $\mu$ g/ml group, 12 h point) was 1259.6-fold of that of control. Similar to that of poly (I:C) group, the transcription of both *bcSTAT1a* and *bcSTAT1b* in MPK cells increased right after LPS treatment (Fig. 2C&D). The highest relative *bcSTAT1a* mRNA level (50  $\mu$ g/ml group, 8 h point) within 48 h post LPS stimulation was 6.7-fold of that of control and the highest relative *bcSTAT1b* mRNA level (50  $\mu$ g/ml group, 24 h point) was 16.5-fold of that of control. As to MPK cells infected with GCRV, the transcription of both *bcSTAT1a* and *bcSTAT1b* increased right after infection (Fig. 3A&B). The highest relative *bcSTAT1a* mRNA level within 48 h post infection (hpf) (1 MOI group, 12 hpf) was 18-fold of that of control, however, the highest relative *bcSTAT1b* mRNA level (1 MOI group, 12 hpf) was 3873.1-fold of that of control. As the downstream component of IFN signaling, *bcSTAT1* transcription in response to bcIFNa stimulation was examined in the MPK cells either treated with bcIFNa-containing media or transfected with plasmid expressing bcIFNa. The transcription of *bcSTAT1a* and *bcSTAT1b* obviously increased after bcIFNa stimulation. The highest increase rate of *bcSTAT1a* mRNA level (28.7-fold of that of control, 4 h point) was obviously lower than that of *bcSTAT1b* mRNA level (894.4-fold of that of control, 4 h point) (Fig. 3C&D). Similar result was seen in MPK cells transfected with plasmid expressing bcIFNa, in which the increase rate of *bcSTAT1a* mRNA level (8.1-fold of that of control) was obviously lower than that of *bcSTAT1b* mRNA level

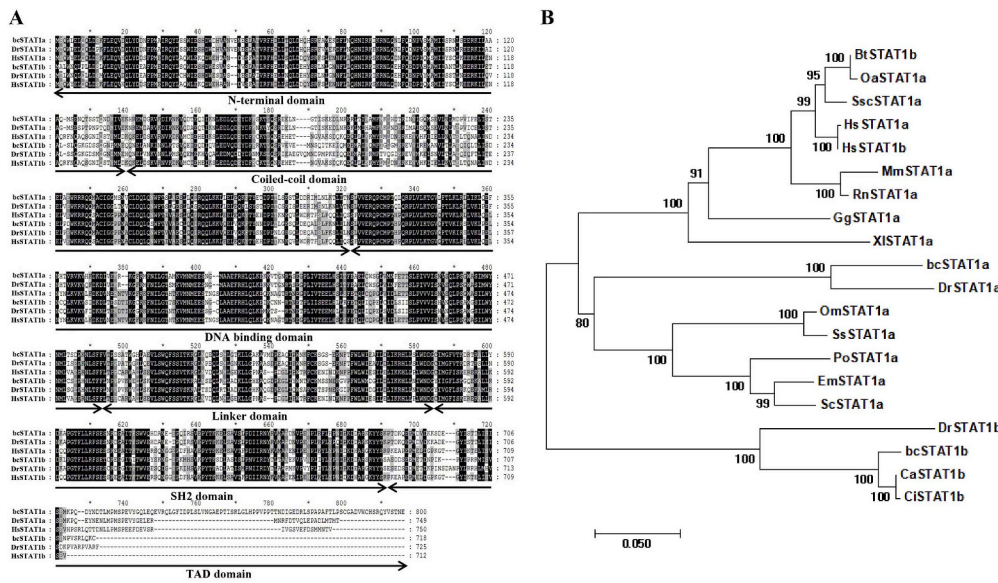


**Fig. 1.** Sequence analysis of bcSTAT1. (A) Comparisons of bcSTAT1 with HsSTAT1 and DrSTAT1. (B) Phylogenetic tree of vertebrate STAT1s. The amino acid sequences of bcSTAT1a and bcSTAT1b were aligned with those of STAT1s from different species by using MEGA 6.0 software, which included (GenBank accession number, unless indicated otherwise): *Bos taurus* (NP\_001071368.1), *Ovis aries* (NP\_001159675.1), *Sus scrofa* (NP\_998934.1), *Homo sapiens* (ADA59516.1 and NP\_644671.1), *Mus musculus* (AAA19454.1), *Rattus norvegicus* (AAF20200.1), *Gallus gallus* (NP\_001012932.1), *Xenopus laevis* (AAM51552.1), *Oncorhynchus mykiss* (NP\_001118179.1), *Salmo salar* (NP\_001117126.1), *Paralichthys olivaceus* (ABS19629.1), *Epinephelus malabaricus* (AGT62457.1), *Siniperca chuatsi* (ACU12484.1), *Danio rerio* (NP\_571555.1 and NP\_956385.2), *Carassius auratus* (AAO88245.1), *Ctenopharyngodon idellus* (ANP93609.1). The bar stands for scale length and the number on different nodes stands for bootstrap value.

**Table 2**  
Comparison of bcSTAT1a and bcSTAT1b with other vertebrate STAT1 (%).

Species	<i>Mylopharyngodon Piceus</i> -1a		<i>Mylopharyngodon Piceus</i> -1b	
	Similarity	Identity	Similarity	Identity
<i>Mylopharyngodon Piceus</i> -1a	100	100	65.0	50.4
<i>Mylopharyngodon Piceus</i> -1b	65.0	50.4	100	100
<i>Danio rerio</i> -1a	86.1	80.7	68.8	53.4
<i>Danio rerio</i> -1b	64.5	48.9	90.1	80.2
<i>Bos taurus</i>	70.2	56.3	75.9	60.3
<i>Carassius auratus</i>	64.9	50.6	99.0	97.6
<i>Ctenopharyngodon idellus</i>	64.8	50.5	98.9	97.4
<i>Epinephelus malabaricus</i>	74.6	61.0	74.3	59.4
<i>Gallus gallus</i>	71.5	58.3	73.6	58.3
<i>Homo Sapiens</i> -1a	72.6	57.8	73.2	58.3
<i>Homo Sapiens</i> -1b	70.4	56.6	75.7	60.2
<i>Mus musculus</i>	71.1	57.5	72.1	58.2
<i>Ovis aries</i>	72.7	57.7	73.5	58.5
<i>Oncorhynchus mykiss</i>	74.3	60.6	74.1	58.8
<i>Paralichthys olivaceus</i>	73.0	59.7	73.8	58.3
<i>Rattus norvegicus</i>	71.9	57.9	73.0	59.2
<i>Siniperca chuatsi</i>	74.9	60.9	74.0	59.5
<i>Salmo salar</i>	74.9	61.1	75.0	59.7
<i>Sus scrofa</i>	71.1	56.4	73.0	57.9
<i>Xenopus laevis</i>	71.9	55.8	72.3	57.1

(1375.6-fold of that of control) (Fig. 3E&F). The q-PCR analysis results demonstrated that *bcSTAT1a* and *bcSTAT1b* transcription increased in response to above stimuli, however, the mRNA level increase rate of *bcSTAT1a* was obviously lower than that of *bcSTAT1b*.

### 3.3. Protein expression and subcellular distribution of bcSTAT1

HEK293T cells and EPC cells were transfected with plasmids expressing bcSTAT1a or bcSTAT1b separately and used for IB assay to investigate the protein expression of bcSTAT1a or bcSTAT1b. In the IB of bcSTAT1a, a specific band of ~95 kDa was detected in the whole cell

lysate of both HEK293T and EPC cells expressing bcSTAT1a which matched the predicted molecular weight of bcSTAT1a (Fig. 4A&C). A faint band slightly bigger (~100 kDa) than the major specific band was detected in the whole cell lysate of HEK293T cells expressing bcSTAT1a, which suggested that this fish protein was modified post translation, most likely phosphorylation. In the IB of bcSTAT1b, a specific band of ~82 kDa was detected in the whole cell lysate of both HEK293T and EPC cells expressing bcSTAT1b, which matched the predicted molecular weight of bcSTAT1b (Fig. 4B&D). Our data demonstrated that bcSTAT1a and bcSTAT1b were well expressed in both mammalian and fish cells. To determine the subcellular distribution of bcSTAT1a and bcSTAT1b, both HEK293T cells and EPC cells were transfected with plasmids expressing bcSTAT1a or bcSTAT1b separately and analyzed by immunofluorescence (IF) staining assay. In the IF data of bcSTAT1a, the brilliant red color representing bcSTAT1a was detected in both cytoplasm and nucleus of both HEK293T and EPC cells. Similar phenomenon was seen in the IF data of bcSTAT1b (Fig. 4E&F), which demonstrated that bcSTAT1a and bcSTAT1b were distributed in both cytoplasm and nucleus. The IF data implied that bcSTAT1a/bcSTAT1b transferred between cytoplasm and nucleus like its mammalian counterparts [11].

### 3.4. The interaction between bcSTAT1a and bcSTAT1b

bcSTAT1a and bcSTAT1b were detected in both cytoplasm and nucleus in the IF assay, which implied bcSTAT1a and bcSTAT1b might possess similar mechanism for their activation like their mammalian counterparts. Thus, the possible interaction between bcSTAT1a and bcSTAT1b was examined by co-IP assay. That bcSTAT1a-HA was precipitated by bcSTAT1a-Flag identified the self-interaction of bcSTAT1a (Fig. 5A). The self-interaction of bcSTAT1b was identified by that bcSTAT1b-HA was precipitated by bcSTAT1b-Flag (Fig. 5B). That bcSTAT1a-HA was precipitated by bcSTAT1b-Flag further identified the direct association between bcSTAT1a and bcSTAT1b (Fig. 5C). A faint band around 92 kDa was detected in the IB of bcSTAT1b-HA (precipitated by bcSTAT1b-Flag), which suggested that bcSTAT1b was modified post translation, most likely modified with phosphorylation. As to that the faint band was not detected in the IB of the whole cell lysate, it could be explained by the low expression level of bcSTAT1b (Fig. 5B).

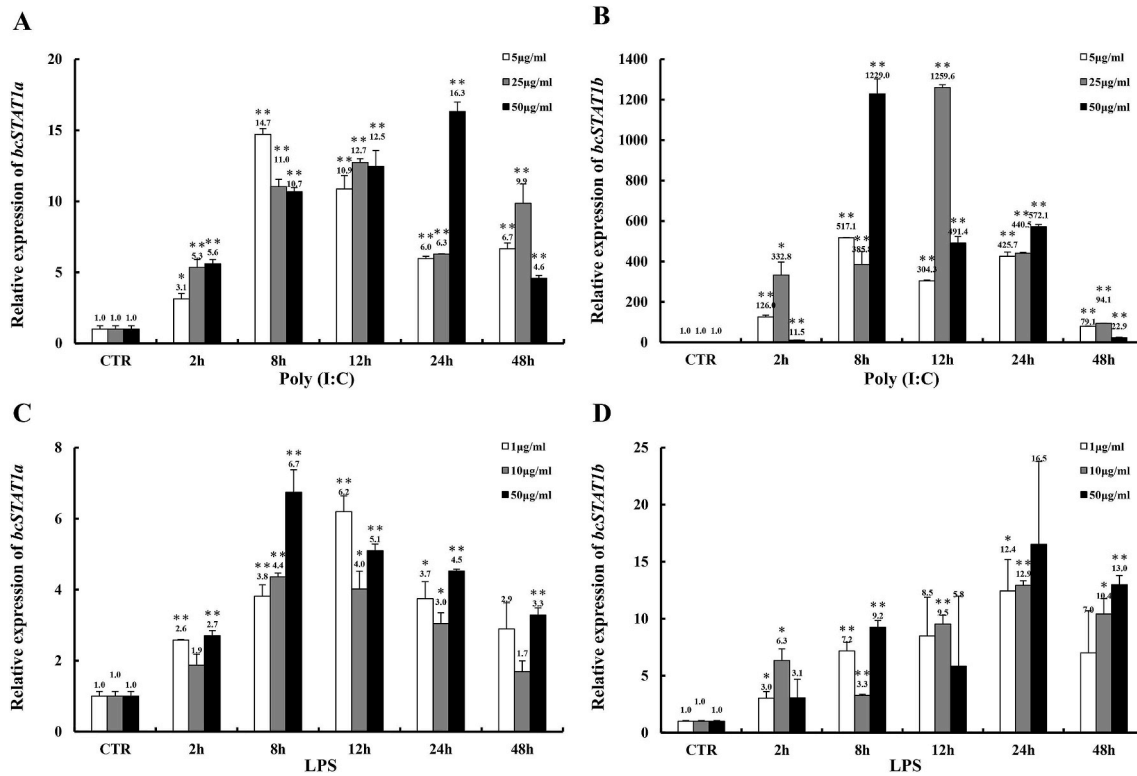


**Fig. 2.** *bcSTAT1* expression *in vitro* in response to poly (I:C) and LPS. MPK cells in 6-well plate ( $2 \times 10^6$  cells/well) were treated with poly (I:C) (A&B) or LPS (C&D) at the indicated concentration separately and harvested for q-PCR at the indicated time points post stimulation independently. The cells without treatment were used as control and the relative mRNA level of *bcSTAT1a* or *bcSTAT1b* of the control was defined as 1. CTR: MPK cells without treatment. The number stands for the average mRNA level of *bcSTAT1a* or *bcSTAT1b*.

To further investigate whether *bcSTAT1a* or *bcSTAT1b* from homodimer or not *in vitro*, HEK293T cells were transfected with plasmids expressing *bcSTAT1a* or *bcSTAT1b* and used for native-PAGE analysis. Both monomer and dimer of *bcSTAT1a* were detected in the IB under non-reduced condition in the whole cell lysate of HEK293T expressing *bcSTAT1a* (Fig. 5D). Similar to that of *bcSTAT1a*, monomer and dimer of *bcSTAT1b* were detected in the IB under non-reduced condition. However, an additional fainter band bigger than the dimer was detected in the whole cell lysate of HEK293T expressing *bcSTAT1b*, which suggested the formation of trimer or tetramer of this protein *in vitro* (Fig. 5E). These data implied that both *bcSTAT1a* and *bcSTAT1b* might form homodimers *in vivo* like their mammalian counterparts.

### 3.5. Antiviral activities of *bcSTAT1a* and *bcSTAT1b*

To investigate whether *bcSTAT1a* or *bcSTAT1b* induces IFN production or not, EPC cells were transfected with plasmids expressing *bcSTAT1a* or *bcSTAT1b* and used for reporter assay separately. The results showed that over-expression of *bcSTAT1a* or *bcSTAT1b* in EPC cells induced *bcIFN $\alpha$*  promoter activity faintly in a dose dependent manner (Fig. 6A&B). Similarly, both exogenous *bcSTAT1a* and *bcSTAT1b* in EPC cells induced zebrafish *INF $\phi$ 3* promoter activity faintly in a dose dependent manner (Fig. 6C&D). The data of reporter assay suggested that both *bcSTAT1a* and *bcSTAT1b* possessed a feedback mechanism for IFN production since these two molecules were down stream of IFN. To clear up the function of *bcSTAT1a* and *bcSTAT1b* in host innate antiviral immune response, EPC cells were transfected with plasmids expressing *bcSTAT1a* or *bcSTAT1b* separately at 24 h before GCRV infection. The plaque assay results showed that the viral titer in the supernatant media of the EPC cells over-expressing *bcSTAT1a* or *bcSTAT1b* was obviously lower than that of the control (Fig. 7A&B). The virus titer in the media of *bcSTAT1a*-expressing cells

presented the biggest reduction to that of control when the cells were infected with GCRV at the dose of 0.1 MOI. The virus titer in the media of *bcSTAT1b*-expressing cells showed the biggest reduction when the cells were infected with GCRV at the dose of 0.01 MOI. Our data demonstrated clearly that both *bcSTAT1a* and *bcSTAT1b* functioned as important antiviral factors in the innate immune response against GCRV.

## 4. Discussion

Mammalian STAT1 plays important roles in the signaling of type I, type II and type III IFNs. In the case of the type I IFN signal pathway, both IFN $\alpha$  and IFN $\beta$  induce the dimerization of type I IFN receptor and activate the associated kinases tyrosine kinase (TYK) 2 and JAK1. Then the phosphorylated JAK1 leads to the tyrosine phosphorylation of STAT1, STAT2 and IRF9, which form a transcription factor complex termed IFN-stimulated gene factor 3 (ISGF3) [13,15,17]. ISGF3 complex translocates into the nucleus and binds to ISREs of ISGs, resulting in the transcriptional activation of ISGs [12]. As to type I IFN signaling of teleost fishes, ISGF3 complex formation is similar to that of mammals. It is interesting that ISGF3 complex only participates in type I IFN signaling pathway in mammals, however, it is recruited into both type I IFN and type II IFN signaling pathways in teleost fishes [34].

STAT1 mediates response to IFNs and regulates some cellular activities in mammals, including innate and adaptive immunity, apoptosis, proliferation and differentiation [40]. Negative regulation of HsSTAT1 $\beta$  inhibited the phosphorylation, DNA binding and transcriptional activity of HsSTAT1 $\alpha$  in B-cells [41]. By contrast, HsSTAT1 $\beta$  in human B-cells was found to be transcriptionally active and capable of eliciting IFN- $\gamma$ -dependent immunity against the bacterium *Listeria monocytogenes* infection *in vivo* [42]. Besides, recent study reported that HsSTAT1 $\beta$  enhanced the expression of HsSTAT1 $\alpha$  and improved its

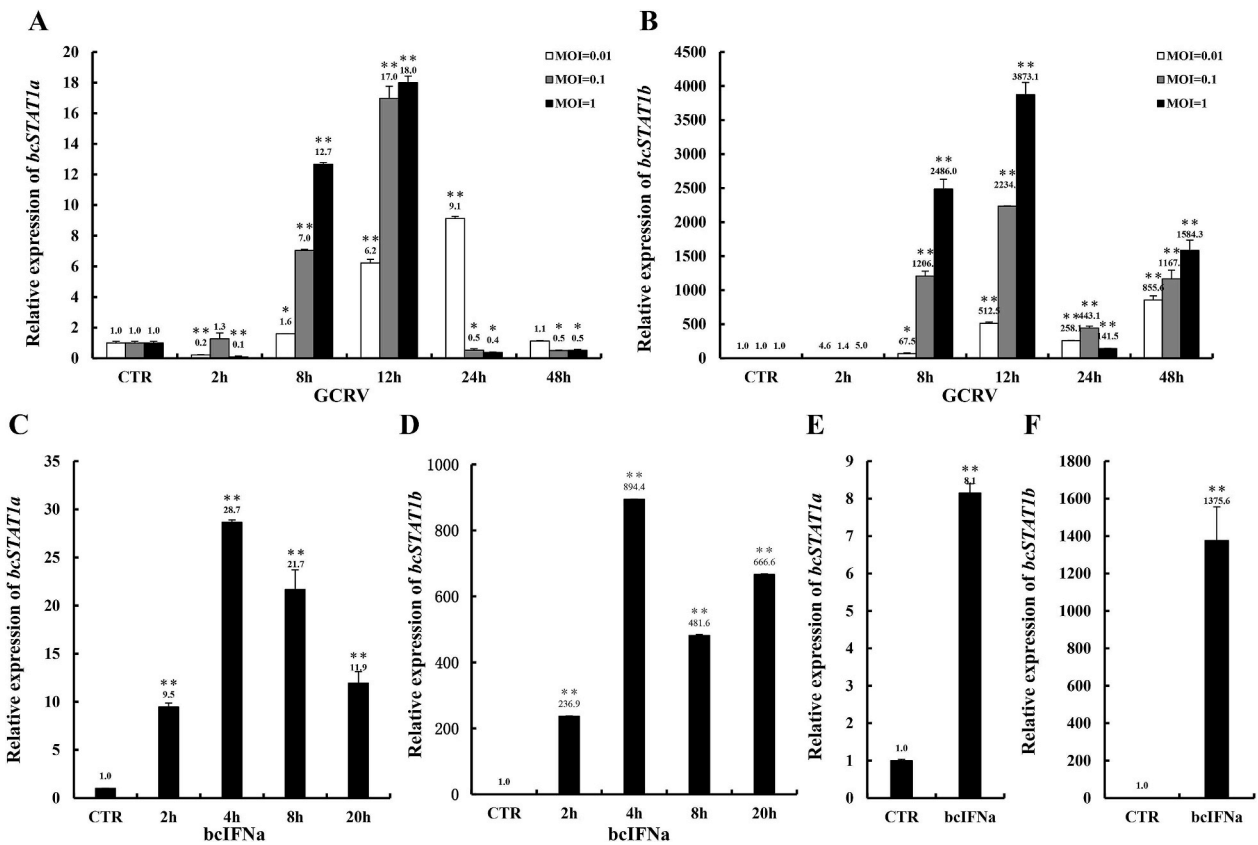


**Fig. 3.** *bcSTAT1* expression *in vitro* in response to GCRV and bcIFN $\alpha$ . MPK cells in 6-well plate ( $2 \times 10^6$  cells/well) were infected with GCRV (A&B) at indicated MOI or treated with bcIFN $\alpha$ -containing media (1.7 ng/ $\mu$ l) separately (C&D) and harvested for q-PCR analysis independently at the indicated time points post stimulation. The cells without treatment were used as control and the relative mRNA level of *bcSTAT1a* or *bcSTAT1b* of the control was defined as 1. CTR: MPK cells without treatment. (E&F) The MPK cells in 6-well plate ( $2 \times 10^6$  cells/well) were transfected with plasmid expressing bcIFN $\alpha$  and harvested for q-PCR analysis. The cells transfected with the empty vectors were used as control and the relative mRNA level of *bcSTAT1a* and *bcSTAT1b* of the control was defined as 1. bcIFN $\alpha$ : pcDNA5/FRT/TO-bcIFN $\alpha$ -HA; CTR: MPK cells transfected with the empty vector. The number stands for the average mRNA level of *bcSTAT1a* or *bcSTAT1b*.

tumor-suppressing function [18]. The interaction between HsSTAT1 $\alpha$  and HsSTAT1 $\beta$  has been characterized by co-IP assay and immunofluorescence staining assay [18]. However, to our knowledge, there is no report about the interaction and antiviral comparison of two STAT1 variants in teleost fishes. In this paper, self-association of bcSTAT1a and bcSTAT1b, and the interaction between bcSTAT1a and bcSTAT1b had been identified through co-IP assay; moreover, both bcSTAT1a and bcSTAT1b showed antiviral activities against GCRV in EPC cells.

*HsSTAT1a* and *HsSTAT1b* are encoded by the same gene that locates in the position of human chromosome Hsa2. However, *DrSTAT1a* and *DrSTAT1b* are from two different genes; *DrSTAT1a* gene locates on zebrafish chromosome Dre9 and *DrSTAT1b* gene locates on zebrafish chromosome Dre22 [27]. *bcSTAT1a* and *bcSTAT1b* are encoded by two black carp *STAT1* genes based on amino acid sequence analysis and phylogenetic analysis. Interestingly, TAD domain is conserved in HsSTAT1 $\alpha$ /*DrSTAT1a*/*bcSTAT1a* but partially missing in HsSTAT1 $\beta$ /*DrSTAT1b*/*bcSTAT1b*. Besides, amino acid sequence of bcSTAT1a is similar to *DrSTAT1a* (86.1%), and that of bcSTAT1b is similar to *DrSTAT1b* (90.1%). Previous report suggested that 25% of human genes had two co-orthologs in zebrafish [43]. Thus, this phenomenon happened in the *STAT1* gene: there were two *STAT1* genes in teleost fishes (both zebrafish and black carp) and a single *STAT1* gene in human.

In the present study, q-PCR data showed that the increase rate of *bcSTAT1b* mRNA level was greatly higher than that of *bcSTAT1a* post different stimulation, which including poly (I:C), GCRV and bcIFN $\alpha$  (Figs. 2 and 3). These results demonstrated that *bcSTAT1a* and *bcSTAT1b* presented the different expression patterns in response to

stimulants challenge, which implied that bcSTAT1b functioned more importantly during host innate immune activation than bcSTAT1a. Interestingly, the transcription levels of *bcSTAT1b* were different between poly (I:C) and LPS (Fig. 2B&D). Poly (I:C) is a synthetic analog of double-stranded RNA (dsRNA), which simulates a molecular pattern associated with viral infection. LPS is an amphiphilic glycolipid of the outer membrane of Gram-negative bacteria, which simulates a molecular pattern associated with bacteria infection. The data suggested that *bcSTAT1b* might be recruited into different mechanisms during innate immune activation after viral or bacteria infection.

Mammalian IFN- $\gamma$  induces the phosphorylated STAT1 to form homodimer in cytoplasm, which transfers into nucleus and activates the transcription of ISGs [14]. It has been reported that HsSTAT1 $\alpha$  translocated the nucleus after it was phosphorylated. In this paper, two bands of bcSTAT1a and two bands of bcSTAT1b had been detected through IB and co-IP (Figs. 4 and 5), which implied that these two black carp STAT1 proteins were modified with phosphorylation. The results of our immunofluorescence assay showed both cytoplasm and nucleus distribution of bcSTAT1a/bcSTAT1b. Thus, it was speculated that bcSTAT1a/bcSTAT1b might possess similar mechanism to be activated and translocated like that of their mammalian counterparts. The co-IP and immunofluorescence assay demonstrated that overexpressed bcSTAT1 was phosphorylated and trans-located into nucleus without stimulation, which could explain that overexpression of bcSTAT1 in EPC cells activated the IFN promoter transcription (Fig. 6). Several proteins and cytokines are able to phosphorylate HsSTAT1 $\alpha$ , which causes an effective antiviral response. Y701, S708 and S727 of HsSTAT1 $\alpha$  are phosphorylated by JAK family members, IKK $\epsilon$  and TLR family members separately

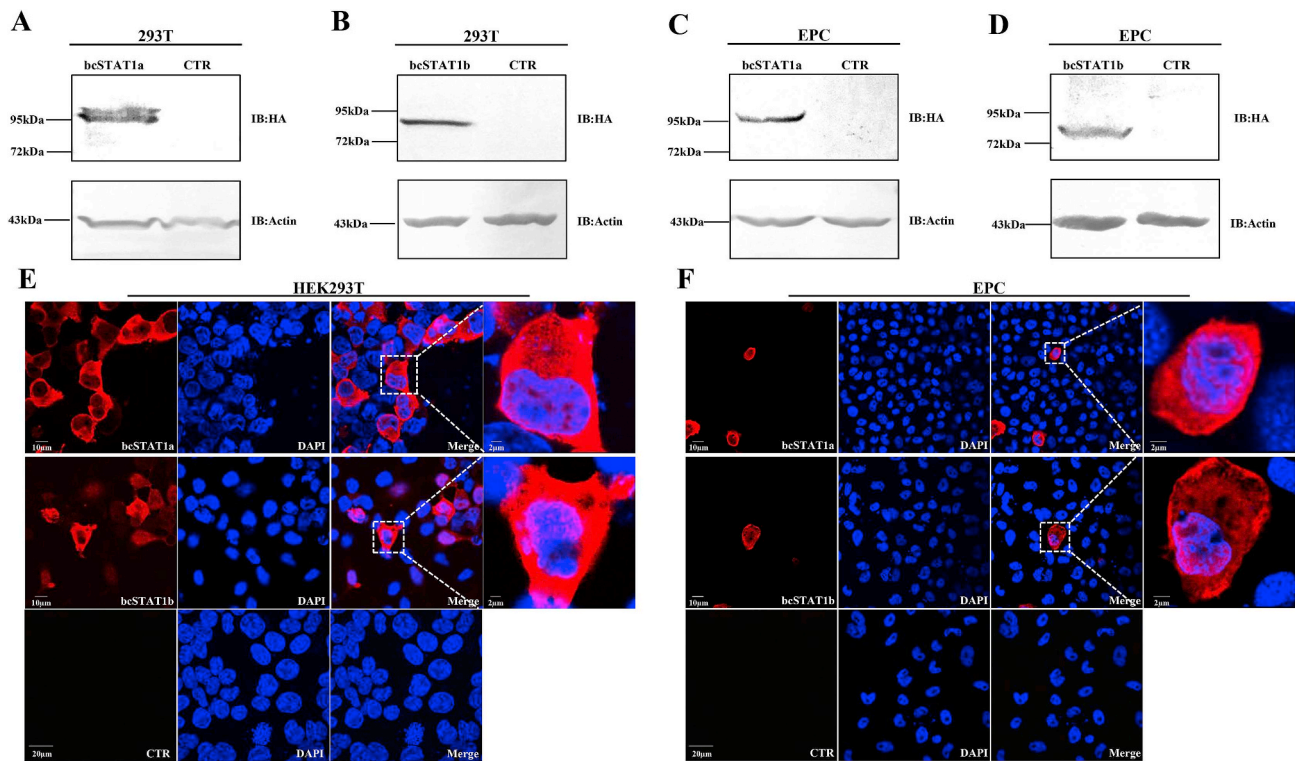


**Fig. 4.** Protein expression and subcellular distribution of bcSTAT1. (A–D) Immunoblot assay of bcSTAT1a and bcSTAT1b in HEK293T cells and EPC cells. IB: immunoblot. CTR: HEK293T or EPC cells transfected with the empty vector. (E&F): Immunofluorescence staining of bcSTAT1a or bcSTAT1b in HEK293T cells and EPC cells; the bars stand for the scale of 2 μm, 5 μm, 10 μm or 20 μm separately. bcSTAT1a: pcDNA5/FRT/TO-bcSTAT1a-HA; bcSTAT1b: pcDNA5/FRT/TO-bcSTAT1b-HA. CTR: HEK293T or EPC cells treated without the primary antibody.

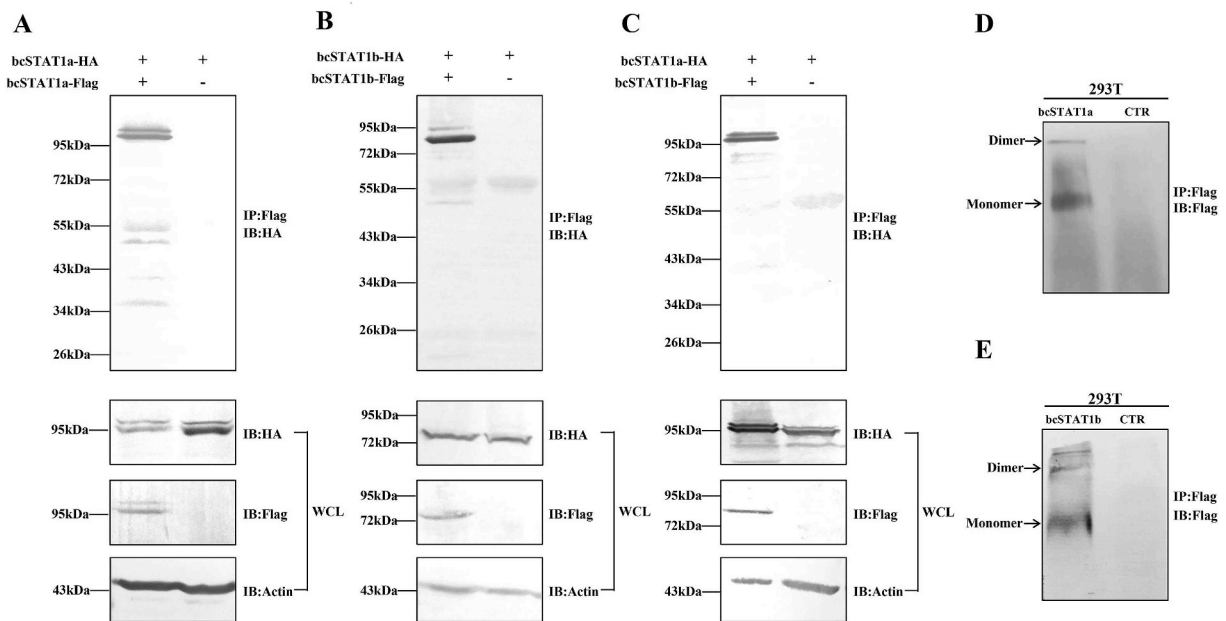


**Fig. 5.** The interaction between bcSTAT1a and bcSTAT1b. HEK293T cells were co-transfected with plasmids expressing bcSTAT1a and/or bcSTAT1b, and the transfected cells were harvested at 48 h post-transfection and lysed for immunoprecipitation. The precipitated proteins either were applied to SDS-PAGE (A, B, C) or native PAGE (D, E) and used for IB assay separately as described in methods. (A) Self-interaction of bcSTAT1a. (B) Self-interaction of bcSTAT1b. (C) The association between bcSTAT1a and bcSTAT1b. WCL: whole cell lysates; bcSTAT1a-HA: pcDNA5/FRT/TO-bcSTAT1a-HA; bcSTAT1a-Flag: pcDNA5/FRT/TO-bcSTAT1a-Flag; bcSTAT1b-HA: pcDNA5/FRT/TO-bcSTAT1b-HA; bcSTAT1b-Flag: pcDNA5/FRT/TO-bcSTAT1b-Flag. IB: immunoblot; IP: immunoprecipitation. CTR: pcDNA5/FRT/TO. (D&E) Dimerization detection of bcSTAT1a or bcSTAT1b. bcSTAT1a: pcDNA5/FRT/TO-bcSTAT1a-Flag; bcSTAT1b: pcDNA5/FRT/TO-bcSTAT1b-Flag.

[11,44,45]. The predicted phosphorylation sites of bcSTAT1a (Y698, S705 and S722) and bcSTAT1b (S706) are similar to those of HsSTAT1a (Y701, S708 and S727) (predicted by NetPhos 3.1 [http://www.cbs.dtu.

dk/services/NetPhos/]). However, whether bcSTAT1a and bcSTAT1b are phosphorylated and the mechanism behind it during host innate immune activation needs to be further explored.

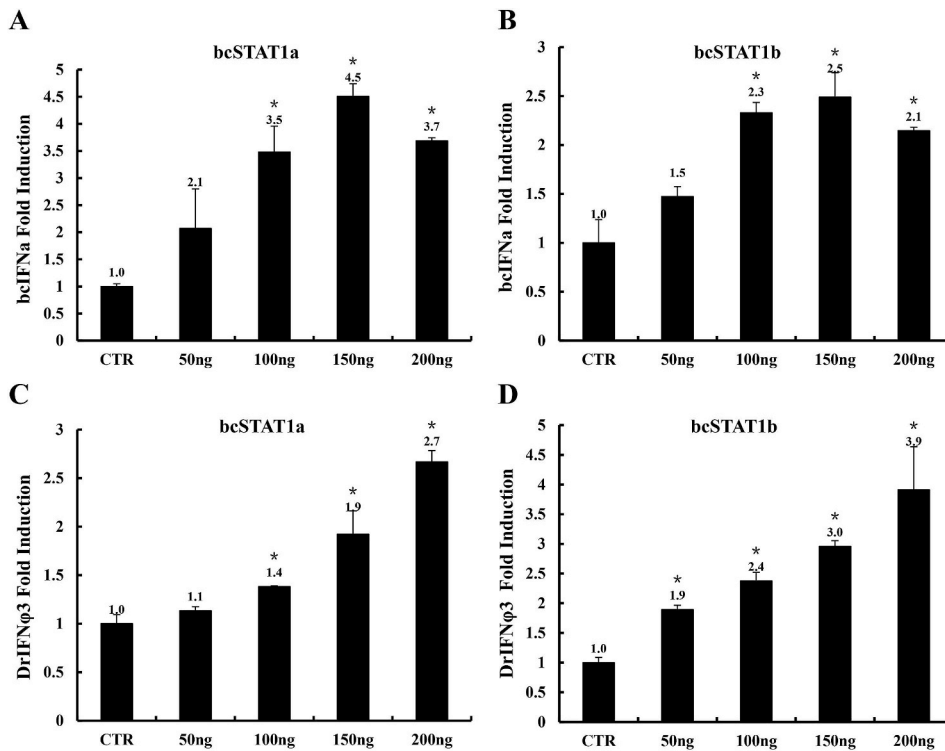


**Fig. 6.** IFN-inducing ability of bcSTAT1. EPC cells in 24-well plate were co-transfected with pRL-TK, Luci-bcIFNα (A&B) or Luci-DrIFNφ3 (C &D) and plasmids expressing bcSTAT1a or bcSTAT1b separately. The relative induced bcIFNα or DrIFNφ3 folds were determined by reporter assay. bcSTAT1a: pcDNA5/FRT/TO-bcSTAT1a-HA; bcSTAT1b: pcDNA5/FRT/TO-bcSTAT1b-HA; CTR: EPC cells transfected with empty vector.

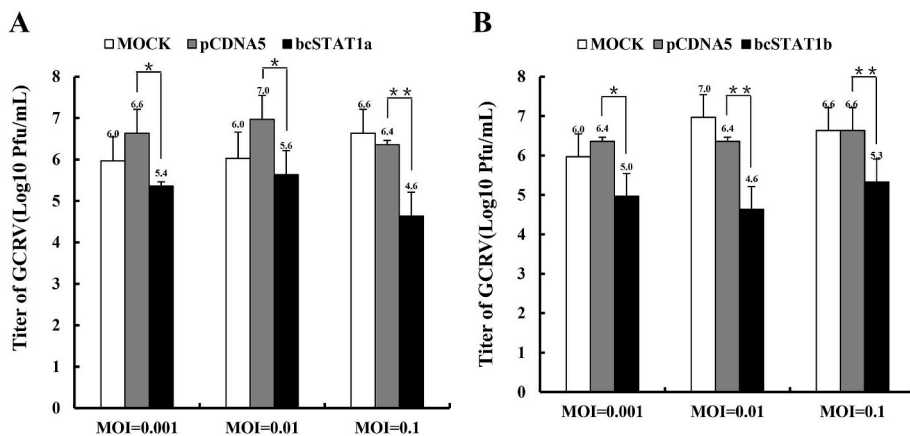


**Fig. 7.** Antiviral activity of bcSTAT1. EPC cells in 24-well plate ( $3 \times 10^5$  cells/well) were transfected with 500 ng plasmids expressing bcSTAT1a (A) or bcSTAT1b (B) separately and infected with GCRV at the indicated MOI at 24 h post transfection. The virus titers in the supernatant media were determined by plaque assay at 48 h post infection. MOCK: EPC cells without transfection, pcDNA5: pcDNA5/FRT/TO, bcSTAT1a: pcDNA5/FRT/TO-bcSTAT1a-HA, bcSTAT1b: pcDNA5/FRT/TO-bcSTAT1b-HA.

**Acknowledgements**

This work was supported by National Natural Science Foundation of China (81471963, 31272634), China Postdoctoral Science Foundation (2018M632970) and the Cooperative Innovation Center of Engineering and New Products for Developmental Biology of Hunan Province (20134486).

**References**

[1] C.A. Thaiss, M. Levy, S. Itav, E. Elinav, Integration of innate immune signaling, *Trends Immunol.* 37 (2016) 84–101.  
 [2] S.N. Chen, P.F. Zou, P. Nie, Retinoic acid-inducible gene I (RIG-I)-like receptors (RLRs) in fish: current knowledge and future perspectives, *Immunology* 151 (2017) 16–25.  
 [3] S.E. Keating, M. Baran, A.G. Bowie, Cytosolic DNA sensors regulating type I interferon induction, *Trends Immunol.* 32 (2011) 574–581.  
 [4] K. Parvatiyar, Z. Zhang, R.M. Teles, S. Ouyang, Y. Jiang, S.S. Iyer, et al., The helicase DDX41 recognizes the bacterial secondary messengers cyclic di-GMP and cyclic di-AMP to activate a type I interferon immune response, *Nat. Immunol.* 13 (2012) 1155–1161.  
 [5] H.H. Shizuo Akira, Recognition of pathogen-associated molecular patterns by TLR family, *Immunol. Lett.* 85 (2003) 85–95.

[6] P. Broz, D.M. Monack, Newly described pattern recognition receptors team up against intracellular pathogens, *Nat. Rev. Immunol.* 13 (2013) 551–565.  
 [7] J. Zou, C.J. Secombes, Teleost fish interferons and their role in immunity, *Dev. Comp. Immunol.* 35 (2011) 1376–1387.  
 [8] R. Benjamin, S.-L.N. tenOever, Mark A. Chua, Sarah M. McWhirter, Adolfo García-Sastre, Tom Maniatis, Multiple functions of the IKK-related kinase IKKε in interferon-mediated antiviral immunity, *Science* 315 (2007) 1274–1278.  
 [9] James E. Darnell Jr., IMK, George R. Stark, Jak-STAT pathways and transcriptional activation in response to IFNs and other extracellular signaling proteins, *Science* 264 (1994) 1415–1421.  
 [10] S.V. Kotenko, G. Gallagher, V.V. Baurin, A. Lewis-Antes, M. Shen, N.K. Shah, et al., IFN-lambdas mediate antiviral protection through a distinct class II cytokine receptor complex, *Nat. Immunol.* 4 (2003) 69–77.  
 [11] B.A.F. Sze-Ling Ng, Sonja Schmid, Jason Gertz, Richard M. Myers, Benjamin R. tenOever, Tom Maniatis, IκB kinase ε (IKKε) regulates the balance between type I and type II interferon responses, *Proc. Natl. Acad. Sci. Unit. States Am.* 108 (2011) 21170–21175.  
 [12] E. David, D.S.K. Levy, Richard Pine, Nancy Reich, E. James, Darnell Jr., Interferon-induced nuclear factors that bind a shared promoter element correlate with positive and negative transcriptional control, *Genes Dev.* 3 (1988) 383–393.  
 [13] E. David, D.S.K. Levy, Richard Pine, E. James, Darnell Jr., Cytoplasmic activation of ISGF3, the positive regulator of interferon-alpha-stimulated transcription, reconstituted in vitro, *Genes Dev.* 3 (1989) 1362–1371.  
 [14] C.S. Ke Shuai, Vincent R. Prezioso, E. James, Darnell Jr., Source. Activation of transcription by IFN-γ. tyrosine phosphorylation of a 91-kD DNA binding protein, *Science* 258 (1992).

- [15] Y. Ren, P. Zhao, J. Liu, Y. Yuan, Q. Cheng, Y. Zuo, et al., Deubiquitinase USP2a sustains interferons antiviral activity by restricting ubiquitination of activated STAT1 in the nucleus, *PLoS Pathog.* 12 (2016) e1005764.
- [16] P.K. Thomas Decker, Anderas Meike, GAS elements: a few nucleotides with a major impact on cytokine-induced gene expression, *J. Interferon Cytokine Res.* 17 (1997) 121–134.
- [17] XinYuan Fu DSK, Susan A. Veals, David E. Levy, J.E. Darnell, J.R. ISGF3, The transcriptional activator induced by interferon alpha, consists of multiple interacting polypeptide chains, *Proc. Natl. Acad. Sci. Unit. States Am.* 87 (1990) 8555–8559.
- [18] Y. Zhang, Y. Chen, H. Yun, Z. Liu, M. Su, R. Lai, STAT1beta enhances STAT1 function by protecting STAT1alpha from degradation in esophageal squamous cell carcinoma, *Cell Death Dis.* 8 (2017) e3077.
- [19] C. Andrew, P.W. Oates, Stephen J. Pratt, Barry H. Paw, Stephen L. Johnson, Robert K. Ho, John H. Postlethwait, Leonard I. Zon, Andrew F. Wilks, Zebrafish stat3 is expressed in restricted tissues during embryogenesis and stat1 rescues cytokine signaling in a STAT1-deficient human cell line, *Dev. Dynam.* 215 (1999) 352–370.
- [20] C.Y. Jung, J. Hikima, M. Ohtani, H.B. Jang, C.S. del Castillo, S.W. Nho, et al., Recombinant interferon-gamma activates immune responses against Edwardsiella tarda infection in the olive flounder, *Paralichthys olivaceus*, *Fish Shellfish Immunol.* 33 (2012) 197–203.
- [21] B. Chinchilla, P. Encinas, A. Estepa, J.M. Coll, E. Gomez-Casado, Transcriptome analysis of rainbow trout in response to non-virion (NV) protein of viral haemorrhagic septicaemia virus (VHSV), *Appl. Microbiol. Biotechnol.* 99 (2015) 1827–1843.
- [22] B. Collet, E.S. Munro, S. Gahlawat, F. Acosta, J. Garcia, C. Roemelt, et al., Infectious pancreatic necrosis virus suppresses type I interferon signalling in rainbow trout gonad cell line but not in Atlantic salmon macrophages, *Fish Shellfish Immunol.* 22 (2007) 44–56.
- [23] B. Collet, N. Bain, S. Prevost, G. Besinque, A. McBeath, M. Snow, et al., Isolation of an Atlantic salmon (*Salmo salar*) signal transducer and activator of transcription STAT1 gene: kinetics of expression upon ISAV or IPNV infection, *Fish Shellfish Immunol.* 25 (2008) 861–867.
- [24] C. Collins, G. Ganne, B. Collet, Isolation and activity of the promoters for STAT1 and 2 in Atlantic salmon *Salmo salar*, *Fish Shellfish Immunol.* 40 (2014) 644–647.
- [25] S. Liu, C. Jiang, C. Duan, L. Hu, S. Zhang, Expression of virus-responsive genes and their response to challenge with poly(I:C) at different stages of the annual fish *Nothobranchius guentheri*: implications for an asymmetric decrease in immunity, *Fish Shellfish Immunol.* 46 (2015) 493–500.
- [26] E.M. Park, J.H. Kang, J.S. Seo, G. Kim, J. Chung, T.J. Choi, Molecular cloning and expression analysis of the STAT1 gene from olive flounder, *Paralichthys olivaceus*, *BMC Immunol.* 9 (2008) 31.
- [27] H. Song, Y.L. Yan, T. Titus, X. He, J.H. Postlethwait, The role of stat1b in zebrafish hematopoiesis, *Mech. Dev.* 128 (2011) 442–456.
- [28] C.H. Tso, Y.F. Hung, S.P. Tan, M.W. Lu, Identification of the STAT1 gene and the characterisation of its immune response to immunostimulants, including nervous necrosis virus (NNV) infection, in malabar grouper (*Epinephelus Malabaricus*), *Fish Shellfish Immunol.* 35 (2013) 1339–1348.
- [29] W.L. Wang, W. Liu, H.Y. Gong, J.R. Hong, C.C. Lin, J.L. Wu, Activation of cytokine expression occurs through the TNFalpha/NF-kappaB-mediated pathway in birnavirus-infected cells, *Fish Shellfish Immunol.* 31 (2011) 10–21.
- [30] J. Zhang, X. Huang, S. Ni, J. Liu, Y. Hu, Y. Yang, et al., Grouper STAT1a is involved in antiviral immune response against iridovirus and nodavirus infection, *Fish Shellfish Immunol.* 70 (2017) 351–360.
- [31] Q.M. Zhang, X. Zhao, Z. Li, M. Wu, J.F. Gui, Y.B. Zhang, Alternative splicing transcripts of zebrafish LGP2 gene differentially contribute to IFN antiviral response, *J. Immunol.* 200 (2018) 688–703.
- [32] Y. Zhang, J. Gui, Molecular characterization and IFN signal pathway analysis of *Carassius auratus* CaSTAT1 identified from the cultured cells in response to virus infection, *Dev. Comp. Immunol.* 28 (2004) 211–227.
- [33] C.H. Cheng, C.M. Chou, C.Y. Chu, G.D. Chen, H.W. Lien, P.P. Hwang, et al., Differential regulation of *Tetraodon nigroviridis* Mx gene promoter activity by constitutively-active forms of STAT1, STAT2, and IRF9, *Fish Shellfish Immunol.* 38 (2014) 230–243.
- [34] M. Sobhkhaz, A. Skjesol, E. Thomassen, L.G. Tollersrud, D.B. Iliev, B. Sun, et al., Structural and functional characterization of salmon STAT1, STAT2 and IRF9 homologs sheds light on interferon signaling in teleosts, *FEBS Open Bio.* 4 (2014) 858–871.
- [35] B.Y. Ruan, S.N. Chen, J. Hou, B. Huang, Z.A. Laghari, L. Li, et al., Two type II IFN members, IFN-gamma and IFN-gamma related (rel), regulate differentially IRF1 and IRF11 in zebrafish, *Fish Shellfish Immunol.* 65 (2017) 103–110.
- [36] J. Xiao, J. Yan, H. Chen, J. Li, Y. Tian, L. Tang, et al., Mx1 of black carp functions importantly in the antiviral innate immune response, *Fish Shellfish Immunol.* 58 (2016) 584–592.
- [37] H. Chen, J. Xiao, J. Li, J. Liu, C. Wang, C. Feng, et al., TRAF2 of black carp upregulates MAVS-mediated antiviral signaling during innate immune response, *Fish Shellfish Immunol.* 71 (2017) 1–9.
- [38] J. Yan, L. Peng, Y. Li, H. Fan, Y. Tian, S. Liu, et al., IFN $\alpha$  of triploid hybrid of gold fish and allotetraploid is an antiviral cytokine against SVCV and GCRV, *Fish Shellfish Immunol.* 54 (2016) 529–536.
- [39] J. Xiao, C. Yan, W. Zhou, J. Li, H. Wu, T. Chen, et al., CARD and TM of MAVS of black carp play the key role in its self-association and antiviral ability, *Fish Shellfish Immunol.* 63 (2017) 261–269.
- [40] K. Meissl, S. Macho-Maschler, M. Muller, B. Strobl, The good and the bad faces of STAT1 in solid tumours, *Cytokine* 89 (2017) 12–20.
- [41] F. Baran-Marszak, J. Feuillard, I. Najjar, C. Le Clorennec, J.M. Bechet, I. Dusanter-Fourt, et al., Differential roles of STAT1alpha and STAT1beta in fludarabine-induced cell cycle arrest and apoptosis in human B cells, *Blood* 104 (2004) 2475–2483.
- [42] N.R.L. Christian Semper, Caroline Lassnig, Matthias Parrini, Tanel Mahlaköiv, Michael Rammerstorfer, Karin Lorenz, Doris Rigler, Simone Müller, Thomas Kolbe, Claus Vogl, Thomas Rüllicke, Staeheli Peter, Thomas Decker, Mathias Müller, Birgit Strobl, STAT1 $\beta$  is not dominant negative and is capable of contributing to gamma interferon-dependent innate immunity, *Mol. Cell Biol.* 34 (2014) 2235–2248.
- [43] H. John, Y.L.Y. Postlethwait, Michael A. Gates, Vertebrate genome evolution and the zebrafish gene map, *Nature* 18 (1998) 354–49.
- [44] K. Luu, C.J. Greenhill, A. Majoros, T. Decker, B.J. Jenkins, A. Mansell, STAT1 plays a role in TLR signal transduction and inflammatory responses, *Immunol. Cell Biol.* 92 (2014) 761–769.
- [45] O. Perwitasari, H. Cho, M.S. Diamond, M. Gale Jr., Inhibitor of kappaB kinase epsilon (IKK(epsilon)), STAT1, and IFIT2 proteins define novel innate immune effector pathway against West Nile virus infection, *J. Biol. Chem.* 286 (2011) 44412–44423.